



VIKAS GROUP OF INSTITUTIONS

(Sponsored by Mother Theresa Educational Society)
Approved by AICTE, New Delhi, PSI, New Delhi & Affiliated to JNTUK,
Kakinada

ISO 9001 : 2015 Certified


Nunna – 521 212, Vijayawada Rural, NTR District, A.P. India.

Email: principal.9t@gmail.com

3.3.1 Number of research papers published per teacher in the Journals as notified on UGC CARE list during

AY 2022

S.No	Title of paper	Name of the author/s	Department of the teacher	Calendar Year of publication
1	Hybrid adder and multiplier based FIR filter design for communication application	G. SEKHAR REDDY	Dept of ECE	2022
2	Development and Validation of a RP-HPLC Method for the Estimation of Remdesivir in Bulk and Pharmaceutical Formulation	POLAREDDY RAJASEKHAR REDDY	Department of Pharmacy	2022
3	Development and Validation of a RP-HPLC Method for the Estimation of Remdesivir in Bulk and Pharmaceutical Formulation	LOKIREDDY MOHAN KRISHNA	Department of Pharmacy	2022
4	Development and Validation of a RP-HPLC Method for the Estimation of Remdesivir in Bulk and Pharmaceutical Formulation	Y.VINAYKUMAR	Department of Pharmacy	2022
5	Investigation on Radiators of 2-Element Array Antenna for Next-Generation Wireless Applications	G. SEKHAR REDDY	Dept of ECE	2022


PRINCIPAL/DIRECTOR
VIKAS GROUP OF INSTITUTIONS
NUNNA - 521 212
Vijayawada Rural, NTR Dist., A.P.

HYBRID ADDER AND MULTIPLIER BASED FIR FILTER DESIGN FOR COMMUNICATION APPLICATIONS

¹TIRUMALASETTI PAVANSAL, ²G. SEK HAR REDDY

¹M.Tech Scholar, Dept of ECE, Vikas Group of institutions, Nunna, Vijayawada A.P, India

²Assistant Professor, Dept of ECE, Vikas Group of institutions, Nunna, Vijayawada A.P, India

ABSTRACT: In this project hybrid adder and multiplier based FIR filter design for communication applications is implemented. The adaptive filter has high throughput whose filter coefficients changes during runtime. The main advantage of FIR Filter is its high computational efficiency. Initially input data is given to D-Flip flop. after that data is shifted in row format. next H-adder and H-Multiplier will perform the addition and multiplication operations. To save this outcome of the system memory controlled filter coefficient is used. PRPG is used to arrange the data in pseudo random pattern and because of this there speed of operation will increases. Hence this project will improve the efficiency in effective way.

KEY WORDS: Analog Filter, Digital Filters, Adaptive Filter, Reconfigurable FIR filter, Memory controlled filter coefficient, PRPG (Pseudo Random Pattern Generator).

I.INTRODUCTION

Each filter in DSP has its own characteristics such as low-pass and high-pass have different type of frequency responses. The parameters like gain, stop-band attenuation, roll-off and oscillations in the responses are different for each filter. All these parameters do not match perfectly with the ideal response characteristics like infinite attenuation in stop-band, faster roll-off and unity pass band gain [1]. In order to obtain ideal characteristics filters optimized using approximation functions in designing of analog linear filter. These approximation functions use statistical methods to optimize the transfer function of the filter being designed. The remarkable characteristics of digital filters in their performance lead to widespread use of them in digital signal processing units.

The two main functions performed by filters in DSP are signal separation and restoration.

If a signal mixed up with interference from other signals or noise, signal separation

would be better choice [2]. For instance, a device recording heart beat of a fetus in the womb. The actual signal interfered by the heartbeat or air inhalation of the mother. In this case, a filter is employed to separate original signals from interfered signals. Therefore, they can be processed separately.

Sometimes signals may lost or distorted due to unusual reasons. In this case, a filter is used to restore the lost signals. Some examples of signal distortion are sounds recorded from a voice recorder of poor standard, blurring of images captured due to imperfect focusing of lens or shaking. The signals distorted in these cases would have been improved using signal restoration filters. Any one of the filter types either analog or digital filters can address this problem [3].

There are many ways for designing of digital filters. Each filter design is suitable for particular application in time-domain or in frequency domain. Filters for the time-domain applications are specially designed to conserve the signal shape because the information is encoded in the signal by the source. Therefore, filters in this domain are employed to preserve the shape of waveforms like signal restoration, suppressing of DC components and smoothing.

Unlike time-domain, the shape of the signal is not significant in frequency domain. Because the signals in the frequency domain contain periodic waveforms, the phase, frequency and amplitude of the signals holds the information. Therefore, filters in this domain are employed to allow certain band of frequencies which holds necessary information. Signal separation is main objective of frequency domain filters [4].

Apart from the filters in two domains other filters are used known as custom filters. The functioning of custom filter is different from the remaining two. This type of custom filters designed to remove the unnecessary convolution that means to perform deconvolution.

Adaptive filter consists of processor, which can be programmed with specific function. The function of the Adaptive filter can be modified by altering program kept inside the memory of a processor, without changing the hardware. Digital filters can be designed, tested and realized effortlessly by using usual computer. The characteristics of analog filters changes with the variations to temperatures. Whereas digital filters are not subjected to changes with time and temperature. Therefore, digital filters stable compared to analog filters.

During previous years, digitals filters are only able process low-frequency signals. Whereas analog filters is best choice for high frequency signals. As the digital technology has been developing without leaps and bounds the frequency range of digital filters increased and can operate in RF frequency range. Unlike limited functionality of analog filters on signals digital filters have special features can process signals in several ways. It makes

Adaptive filter adaptable to variations in the properties of the signal [5].

Digital filters can achieve hard targets of filter characteristics with the help composite arrangements of filters such as series or parallel. These designs are much easier and compressed rather than analog filters.

II. BACKGROUND OF FILTERS

In analog filters the filtering characteristics are achieved using some electronic elements like capacitors, resistors and operational amplifiers. This kind of analog filter is employed in noise suppression, graphic equalizers, video enhancement and wireless network systems. An analog filter to perform specific function can be implemented using some well-known organized methods. Analog filters are employed for signals, which are continuously varying quantities (ex: voice signals from a recorder, current or voltage outputs from transducers)

In digital filters the filtering characteristics are achieved by performing mathematical operations on the sampled values of digital signal. It employs a conventional processor or specific signal-processing chip. In DSP processors initially the analog signal is changed into digital format using ADC (analog to digital converter). The continuous signal is sampled and then quantized to make a digital signal.

The signal produced consists of consecutive samples indicating different input signals values in the form of binary numbers. The next stage processor in Adaptive filter performs various mathematical operations on the transformed digital signal. These operations may include multiplication by some constants and adding the resultant product values. The resultant signal also consists of modified sampled values, which undergo digital to analog conversion by

DAC. Instead of continuous signals like voltage or current, Adaptive filter processes the signals. Which are present in the form of samples indicating binary numbers.

There are many ways for designing of digital filters. Each filter design is suitable for particular application in time-domain or in frequency domain. Filters for the time-domain applications are specially designed to conserve the signal shape because the information is encoded in the signal by the source. Therefore, filters in this domain are employed to preserve the shape of waveforms like signal restoration, suppressing of DC components and smoothing.

Unlike time-domain, the shape of the signal is not significant in frequency domain. Because the signals in the frequency domain contain periodic waveforms, the phase, frequency and amplitude of the signals holds the information. Therefore, filters in this domain are employed to allow certain band of frequencies which holds necessary information. Signal separation is main objective of frequency domain filters.

Apart from the filters in two domains other filters are used known as custom filters. The functioning of custom filter is different from the remaining two. This type of custom filters designed to remove the unnecessary convolution that means to perform de-convolution. These are three types of filter according to their use. We can classify filters in other way based on the filter structure exploited for realization of the filters. The classification of filters according to the differential equation and structure are given as

- Linear and Non linear
- Time invariant and Time varying
- Adaptive and Non adaptive
- Recursive and non-recursive

III. PROPOSED SYSTEM

The below figure (4.2) shows the block diagram of proposed system. Initially input data is given to D-Flip flop. after that data is shifted in row format. next H-adder and H-Multiplier will perform the addition and multiplication operations. To save this outcome of the system memory controlled filter coefficient is used. PRPG is used to arrange the data in pseudo random pattern and because of this there speed of operation will increases.

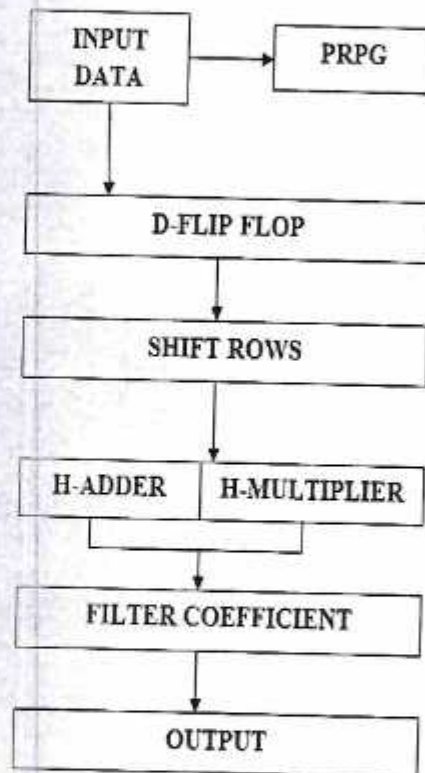


Fig. 1: BLOCK DIAGRAM OF PROPOSED SYSTEM

Initially, the input signal is followed by the data acquisition block. The main intent of data acquisition block is convert the signal into data. This data is modified by the addition of entities at one end of sequence and removal of entities from other end sequence.

Signature

The Memory controlled Filter coefficient is another sort of successive rationale circuit that can be utilized for the capacity or the exchange of twofold information. This successive gadget stacks the information present on its data sources and afterward Shift s or "Shift s" it to its yield once every clock cycle, thus the name Shift Register.

The term 'adaptive' refers to acquiring one's behavior. A filter is said to be adaptive filter, if it has the capability to adjust according to the characteristics of the input signal. Adaptive filters are significant in various applications of DSP like noise suppression, termination of echoes in phones, signal enhancement in medical diagnosis and control systems. Adaptive filters are feasible to employ for the signals which are changing continuously. When a signal is changing its characteristics continuously the noise also varies with the time and the amount interference by the noise in the varying signal is cannot be determined accurately. The effective suppression of noise takes place only if the filter has ability to adjust to the signal. Consider a frequency spectrum of a signal which has strong noise interference. In this case filtering by using a conventional filter will not conserve the shape of the signal.

One of the widely used filters among different classes of digital filters is moving average filter. It is a widely used filter due to ease of implementation and the ability to suppress the random noise. Moving average filter is a superior filter among all time-domain filter, because it preserves the edges of step response during its filtering operation. The frequency domain characteristics of the moving average filter is contrast to the time-domain. This filter cannot separate frequencies appropriately. Some other filters like Gaussian, Blackman filters show improvement in response

characteristics than moving average but, at a cost of high calculation time

IV. RESULTS

The below figure (3) & (4) shows the RTL schematic and technology schematic of Proposed system. RTL schematic is the combination of inputs and outputs.

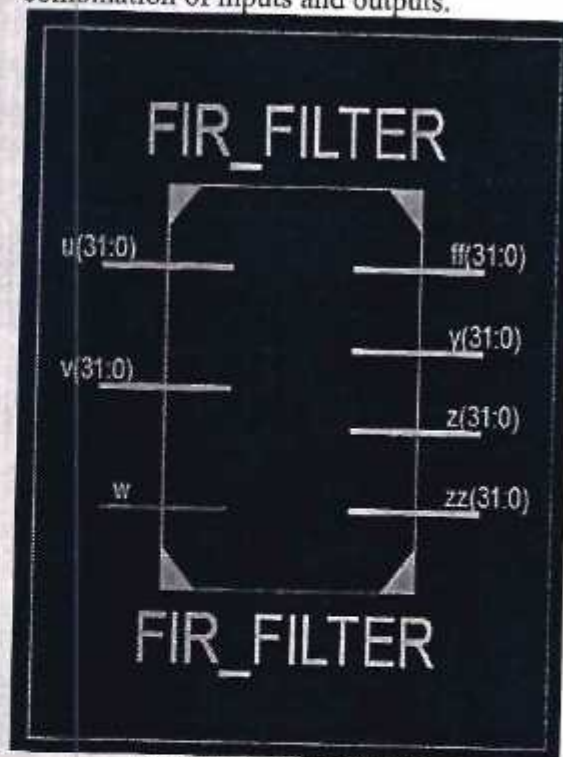


Fig. 2: RTL SCHEMATIC

Technology schematic is the combination of Look up tables, Truth Tables, K-Map and equations



Fig. 3: TECHNOLOGY SCHEMATIC

ASSKORE



Fig. 4: OUTPUT WAVEFORM
V. CONCLUSION

Hence in this paper hybrid adder and multiplier based FIR filter design for communication applications is implemented. The adaptive filter has high throughput whose filter coefficients changes during runtime. The main advantage of FIR Filter is its high computational efficiency. Initially input data is given to D-Flip flop. After that data is shifted in row format. next H-adder and H-Multiplier will perform the addition and multiplication operations. To save this outcome of the system memory controlled filter coefficient is used. PRPG is used to arrange the data in pseudo-random pattern and because of this there speed of operation will increases. Hence this project will improve the efficiency in effective way.

VI. REFERENCES

- [1] Zheng, wei zheng, "FIR filter design based on FPGA", 2018 international conference on measuring technology.
- [2] Atul A. Chandekar, Mahesh Pawar, "Delay and Power Optimized Adaptive Filter using Distributed Arithmetic", 978-1-5090-5686-6/17/\$31.00 ©2017 IEEE.
- [3] Mphd Tasleem Khan, Shaik Rafi Ahamed, "Low Complexity and Critical Path based VLSI Architecture for LMS Adaptive Filter using Distributed Arithmetic", 2017 30th International Conference on VLSI Design and 2017 16th

International Conference on Embedded Systems.

- [4] C S Vinitha, R K Sharma, "Memory-Based VLSI Architectures for Digital Filters: A Survey", 978-1-5090-5384-1/16/\$31.00 ©2016 IEEE.
- [5] Subrahmanyam Mula, Vinay Chakravarthi Gogineni, and Anindya Sundar Dhar, "Robust Proportionate Adaptive Filter Architectures Under Impulsive Noise", 1063-8210 © 2014 IEEE.
- [6] Vakulabharanam Ramakrishna, Tipparti Anil Kumar, "Low Power VLSI Implementation of Adaptive Noise Canceller Based on Least Mean Square Algorithm", 2013 4th International Conference on Intelligent Systems, Modelling and Simulation.
- [7] K.Deergha Rao, Ch..Gangadhar, "VLSI Realization of Adaptive Equalizers of SIMO FIR Second Order Volterra Channels", 1-4244-0387-1/06/\$20.00 © 2006 IEEE.
- [8] Ming-Hwa Sheu, Ho-En Liao, Shih-Tsung Kim, Ming-Der Shieh, "A Novel Adaptive Algorithm and VLSI Design for Frequency Detection in Noisy Environment Based on Adaptive ITR Filter", 0-7803-6685-9/01/\$10.00©2001 IEEE.
- [9] Alejandro Diaz-Sanchez and Jaime Ramirez-Angulo, "A Novel VLSI Sampled-Data Adaptive Filter", 0-7803-3583-X/97 \$10.00 01997 IEEE.
- [10] Alejandro Dim-Sanchez" and Jaime Ramirez-Angulon, "VLSI Voltage Mode FIR Analog Adaptive Filters", 0-7803-3636-4/97 \$10.00 0 1997 IEEE.
- [11] L. Zhao, W. H. Bi, F. Liu, "Design of digital FIR bandpass filter using distributed algorithm based on FPGA," Electronic Measurement Technology, 2007, vol. 30, pp.101-104.
- [12] H. Chen, C. H. Xiong, S. N. Zhong, "FPGA-based efficient programmable polyphase FIR filter," Journal of Beijing Insitute of Technology, 2005, vol. 14, pp. 4-8.

- [13] Y. T. Xu, C. G. Wang, J. L. Wang, "Hardware Implementation of FIR Filter Based on DA Algorithm," Journal of PLA University of Science and Technology, 2003, vol. 4, pp. 22-25.
- [14] D. Wu, Y. H. Wang, H. Z. Lu, "Distributed Arithmetic and its Implementation in FPGA," Journal of National University of Defense Technology, 2000, vol. 22, pp.16-19.
- [15] L. Wei, R. J. Yang, X. T. Cui, "Design of FIR filter based on distributed arithmetic and its FPGA implementation, " Chinese Journal of Scientific Instrument, 2008, vol. 29, pp. 2100-2104.



Development and validation of a RP-HPLC Method for the Estimation of Remdesivir in Bulk and Pharmaceutical Formulation

Polareddy Rajasekhar Reddy, Lokireddy Mohan Krishna*, Y. Vinay Kumar

Department of Pharmacy, Vikas group of institutions, Nunna, Vijayawada rural, Andhra Pradesh- 521212, India.

Corresponding Author: Lokireddy mohan Krishna

ABSTRACT

A simple, reproducible and efficient reversed phase high performance liquid chromatographic (RP-HPLC) method has been developed for estimation of the broad-spectrum antiviral prodrug, Remdesivir in raw material and its injection dosage form. Separation was done by using mobile phase consisting of Acetonitrile : 0.1% Triethylamine, TEA (70:30). The separations were carried out on a Column X-Bridge phenyl (150x4.6mm, 3.5 μ) at a flow rate of 1 mL/min. The injection volume was 10 μ l and the peaks were detected at 235 nm. The linear dynamic response was found to be in the concentration range of 50 μ g/mL-300 μ g/mL, and coefficient of correlation was found to be 0.9989. The %RSD value was below 2.0 μ g/mL for intraday and interday precision indicated that the method was highly precise. The LOD and LOQ were found to be 6.0 μ g/mL, and 20 μ g/mL, respectively which revealed that the method was highly sensitive. The percentage recovery value was higher than 100 %, indicating the accuracy of the method and absence of interference of the excipients present in the formulation. The proposed method was simple, fast, accurate, precise and reproducible and hence can be applied for routine quality control analysis of Remdesivir in bulk and pharmaceutical formulation.

Keywords: Remdesivir, Estimation, Injection, RP-HPLC.

INTRODUCTION

Remdesivir is a broad-spectrum antiviral medication. It is administered via injection into a vein. During the COVID-19 pandemic, Remdesivir was approved or authorized for emergency use to treat COVID-19 in numerous countries. Remdesivir was originally developed to treat hepatitis

C⁽¹⁷⁾, and was subsequently investigated for Ebola virus disease and Marburg virus infections⁽¹⁸⁾ before being studied as a post-infection treatment for COVID-19⁽¹⁹⁾. Remdesivir is a prodrug that is intended to allow intracellular delivery of GS-441524 monophosphate and subsequent biotransformation into GS-441524 triphosphate, a ribonucleotide analogue inhibitor of viral RNA polymerase⁽¹⁴⁾.

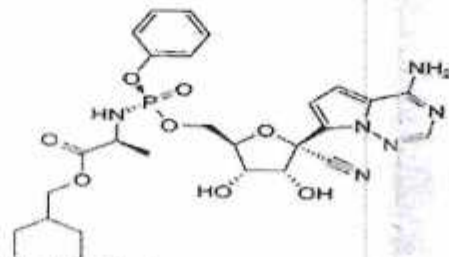


Fig 1: Molecular structure of Remdesivir

MSR
PRINCIPAL/DIRECTOR
VIKAS GROUP OF INSTITUTIONS
NUNNA, - 521 212
Vijayawada Rural, NTR Dist., A.P.



Development and validation of a RP-HPLC Method for the Estimation of Remdesivir in Bulk and Pharmaceutical Formulation

Polareddy Rajasekhar Reddy, Lokireddy Mohan Krishna*, Y. Vinay Kumar

Department of Pharmacy, Vikas group of institutions, Nunna, Vijayawada rural, Andhra Pradesh- 521212, India.

Corresponding Author: Lokireddy mohan Krishna

ABSTRACT

A simple, reproducible and efficient reversed phase high performance liquid chromatographic (RP-HPLC) method has been developed for estimation of the broad-spectrum antiviral prodrug, Remdesivir in raw material and its injection dosage form. Separation was done by using mobile phase consisting of Acetonitrile : 0.1% Triethylamine, TEA (70:30). The separations were carried out on a Column X-Bridge phenyl (150x4.6mm, 3.5 μ) at a flow rate of 1 mL/min. The injection volume was 10 μ l and the peaks were detected at 235 nm. The linear dynamic response was found to be in the concentration range of 50 μ g/mL-300 μ g/mL, and coefficient of correlation was found to be 0.9989. The %RSD value was below 2.0 μ g/mL for intraday and interday precision indicated that the method was highly precise. The LOD and LOQ were found to be 6.0 μ g/mL, and 20 μ g/mL, respectively which revealed that the method was highly sensitive. The percentage recovery value was higher than 100 %, indicating the accuracy of the method and absence of interference of the excipients present in the formulation. The proposed method was simple, fast, accurate, precise and reproducible and hence can be applied for routine quality control analysis of Remdesivir in bulk and pharmaceutical formulation.

Keywords: Remdesivir, Estimation, Injection, RP-HPLC.

INTRODUCTION

Remdesivir is a broad-spectrum antiviral medication. It is administered via injection into a vein. During the COVID-19 pandemic, Remdesivir was approved or authorized for emergency use to treat COVID-19 in numerous countries. Remdesivir was originally developed to treat hepatitis

C¹⁷, and was subsequently investigated for Ebola virus disease and Marburg virus infections^[18] before being studied as a post-infection treatment for COVID-19^[19]. Remdesivir is a prodrug that is intended to allow intracellular delivery of GS-441524 monophosphate and subsequent biotransformation into GS-441524 triphosphate, a ribonucleotide analogue inhibitor of viral RNA polymerase^[14].

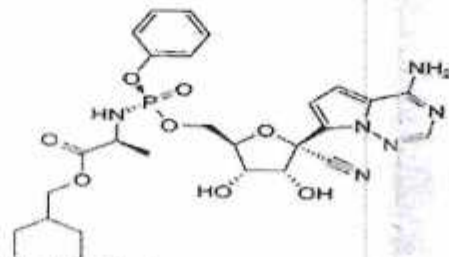


Fig 1: Molecular structure of Remdesivir

M. S. Reddy
PRINCIPAL/DIRECTOR
VIKAS GROUP OF INSTITUTIONS
NUNNA, - 521 212
Vijayawada Rural, NTR Dist., A.P.



Development and validation of a RP-HPLC Method for the Estimation of Remdesivir in Bulk and Pharmaceutical Formulation

Polareddy Rajasekhar Reddy, Lokireddy Mohan Krishna*, Y. Vinay Kumar

Department of Pharmacy, Vikas group of institutions, Nunna, Vijayawada rural, Andhra Pradesh- 521212, India.

Corresponding Author: Lokireddy mohan Krishna

ABSTRACT

A simple, reproducible and efficient reversed phase high performance liquid chromatographic (RP-HPLC) method has been developed for estimation of the broad-spectrum antiviral prodrug, Remdesivir in raw material and its injection dosage form. Separation was done by using mobile phase consisting of Acetonitrile : 0.1% Triethylamine, TEA (70:30). The separations were carried out on a Column X-Bridge phenyl (150x4.6mm, 3.5 μ) at a flow rate of 1 mL/min. The injection volume was 10 μ l and the peaks were detected at 235 nm. The linear dynamic response was found to be in the concentration range of 50 μ g/mL-300 μ g/mL, and coefficient of correlation was found to be 0.9989. The %RSD value was below 2.0 μ g/mL for intraday and interday precision indicated that the method was highly precise. The LOD and LOQ were found to be 6.0 μ g/mL, and 20 μ g/mL, respectively which revealed that the method was highly sensitive. The percentage recovery value was higher than 100 %, indicating the accuracy of the method and absence of interference of the excipients present in the formulation. The proposed method was simple, fast, accurate, precise and reproducible and hence can be applied for routine quality control analysis of Remdesivir in bulk and pharmaceutical formulation.

Keywords: Remdesivir, Estimation, Injection, RP-HPLC.

INTRODUCTION

Remdesivir is a broad-spectrum antiviral medication. It is administered via injection into a vein. During the COVID-19 pandemic, Remdesivir was approved or authorized for emergency use to treat COVID-19 in numerous countries. Remdesivir was originally developed to treat hepatitis

C¹⁷, and was subsequently investigated for Ebola virus disease and Marburg virus infections^[18] before being studied as a post-infection treatment for COVID-19^[19]. Remdesivir is a prodrug that is intended to allow intracellular delivery of GS-441524 monophosphate and subsequent biotransformation into GS-441524 triphosphate, a ribonucleotide analogue inhibitor of viral RNA polymerase^[14].

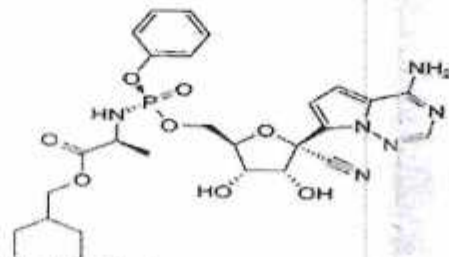


Fig 1: Molecular structure of Remdesivir

MSR
PRINCIPAL/DIRECTOR
VIKAS GROUP OF INSTITUTIONS
NUNNA, - 521 212
Vijayawada Rural, NTR Dist., A.P.

Investigation on Radiators of 2-Element Array Antenna for Next-Generation Wireless Applications



Ch. Murali Krishna, M. Rama Krishna, Siragam Srilali, G. Sekhar Reddy, and B. Anitha Pravalli

Abstract This paper presents 2-element array antenna which is composed with various types of radiators such as rectangular shape element, octagon shape element and hybrid shape element for radio frequency identification (RFID) systems, millimeter wave (mm) next-generation wireless (NGW) applications such as fifth generation, remote sensing, satellite and military applications. Proposed antenna has been designed on Rogers RT/Duroid 5880 (tm) dielectric material ($\epsilon_r = 2.2$, $\tan \delta = 0.0008$), and overall dimension of designed antennas is 10 mm x 6 mm x 0.508 mm. Simulation results of proposed antenna offers dual resonances in Ka - band (26.5 - 40GHz). Realized peak gains and reflection coefficient of designed antennas are 8.01 dBi and - 24.35 dB at 30.05 GHz, 7.69 dBi and - 23.20 dB at 38.70 GHz for rectangular elements; 9.54 dBi and - 35.33 dB at 31 GHz, 9.84 dBi and - 12.86 dB at 40.30 GHz for octagon elements; 8.96 dBi and - 36.18 dB at 30.9 GHz, 9.51 dBi and - 15.38 dB at 39.8 GHz for hybrid radiator elements is obtained, respectively. The proposed antenna is fed by transmission line.

Keywords 2-element array · Different radiators · Line feed · Dual band · Gain · Group delay · NGW applications

Ch. Murali Krishna (✉)
Department of ECE, PDPM IIIT Design and Manufacturing, Jabalpur 482005, India

M. Rama Krishna
Department of ECE, Ramachandra College of Engineering, Eluru 534007, India
e-mail: Ramakrishna05419@rcee.ac.in


S. Srilali
Department of ECE, Swarnandhra College of Engineering & Technology, Nursapur 534280, India

G. Sekhar Reddy
Department of ECE, Vikas Group of Institutions, Nunna 521212, India

B. Anitha Pravalli
Department of ECE, Aditya College of Engineering and Technology, Surampalem 533291, India

© The Author(s), under exclusive license to Springer Nature Singapore Pte Ltd. 2022
A. P. Pandian et al. (eds.), *Proceedings of Third International Conference on Intelligent Computing, Information and Control Systems, Advances in Intelligent Systems and Computing* 1415, https://doi.org/10.1007/978-981-16-7330-6_34

445


PRINCIPAL/DIRECTOR
VIKAS GROUP OF INSTITUTIONS
NUNNA - 521 212
Vijayawada Rural, NTR Dist., A.P

1 Introduction

The communication is increasing day by day; there is advancement in the technology. So, the devices are able to work for longer distances and also at higher frequencies. Nowadays, the higher range frequencies receive an attention due to its potential benefits for the advanced applications. For this purpose, array of antennas in which multiple antennas are combined to single will work like single antenna and achieves the desired directional purpose. While in single antenna, all elements individually radiate, in array antenna for getting radiation, all elements will get sum up; this will increase the overall gain of the antenna and also performance of the antenna, and the losses will be less. As in the same way of dipole, a driven element acts as the transmitter or else a receiver; from a transmitter, a driven element gets power directly when the transmission line is connected. This array of antennas can be obtained in many forms as a linear, circular. The applications which mostly used were in the radar communication and in wireless communication [1–17].

In this paper [1], a microstrip antenna was designed and fabrication with which it is millimeter (mm) and the substrate used was Rogers/RT Duroid 5880 (tm) which covers the frequency in the range of 39.6 GHz and the resonance frequency in the range of 37.30–41.45 GHz and the bandwidth percentage was about 10.53%, and the size of the antenna was $12.5 \times 6 \times 0.508 \text{ mm}^3$ and the applications of this NGS. In [2], the simulated antenna design was about 4×4 array as it is a wideband which covers in the range of about 60GHz. For increasing impedance bandwidth L-Shaped probe fed improved the impedance bandwidth up to 25.5% of designed antenna; which is linearly polarized, produces gain 15.2dBi and also it exhibits the circularly polarized, obtained gain 14.5dBi and the bandwidth was about 17.8%. In this paper [3], a dual band antenna was designed and fabricated within size $65 \times 65 \times 1.6 \text{ mm}^3$ for the applications of Global positioning system and SDAR's and the dual polarizations exist in the frequency covers in the range of about 1.1764 GHz and 2.3325 GHz. In this [6] design, the overall size of the antenna was about $43 \text{ mm} \times 104 \text{ mm} \times 14.5 \text{ mm}$ and its efficiency is better 80%, and impedance matching is less than -10 dB . For the SDARs, the gain was about 5.8 dBi. In this [7], L - Shaped patches and tapered elliptical cavity loaded circularly polarized antenna covers frequency range of 56.9 to 63.4 GHz and achieved gain is 10.4 dBi to excite orthogonal modes LSP's are fed on the metal surface of the substrate in traverse. In this design [8], the size of the antenna is about $87 \times 87 \times 4.572 \text{ mm}^3$ in which it is circularly polarized, and it is fabricated the bandwidth about in the frequency range of 35 MHz, and the simulated gain is about 4.5 dBi. In this paper [14] for the purpose of 5G applications, a dual band MIMO was proposed in which it is a 6-element which covers the frequency in the range of 4–20 dB the isolation which is maximum about $-27/-28 \text{ dB}$. For the future of 5G, mm-wave PIFA was used. In this paper [15], a microstrip patch antenna was designed with the multiple slots for the applications of WiMAX and also WLAN in which its frequency covers in the frequency range of 2.7–3.8 and 5.4–6 GHz.



PRINCIPAL/DIRECTOR
VIKAS GROUP OF INSTITUTIONS
NUNNA - 521 212
Vijayawada Rural, NTR Dist., A.P

In this paper, various radiators are implemented on 2-element array antenna for developing high impact dual resonances, which are applicable for next-generation applications in Ka-band (26.5–40 GHz) region. Proposed antenna has additional advantages such as low weight, smaller in size, cost effective and easier design. Performance of designed antennas is investigated in terms of reflection coefficient, VSWR, group delay, 3D gain plots, 2D radiation patterns and current distribution on radiating elements. Rest of the paper is described as follows: Sect. 2 explains the 2-element array antenna loaded with rectangular, octagon and hybrid radiator design configurations and results discussion. Design summary of designed antennas are reported in Sect. 3. Finally, Sect. 4 concludes the paper.

2 Antenna Design Configuration and Results Discussion

The proposed antennas are designed on Rogers RT/Duroid 5880 (tm) with dielectric constant (ϵ_r) = 2.2, loss tangent ($\tan \delta$) = 0.0008 and its thickness (h) is 0.508 mm. The designed antennas are simulated using high-frequency structure simulator (HFSS) electromagnetic computational tool. Designed antennas are composed of two radiating elements with transmission line feeding and interconnected with strip lines to improve the performance of designed antenna. In this paper, different shapes of radiating elements are designed for investigating the performance of 2-element array antenna for millimeter wave next-generation wireless (NGW) applications over Ka-band (26.5–40 GHz). The suggested 2-element array antenna is smaller in size, easy to fabricate, low profile and light weight.

2.1 Design and Discussion About 2-Element Array Antenna Loaded with Rectangular Elements

Figure 1 shows the 2-element array antenna composed of rectangular radiators printed on one side of dielectric material Rogers RT/Duroid 5880 (tm), and other side is full ground plane. Dimensions of the rectangular radiators are optimized and measured from standard microstrip antenna design equations [12]. Geometrical parameters represented on designed antenna are $L_{sub} = 6$ mm, $W_{sub} = 10$ mm, $L_f = 1.5$ mm, $W_f = 0.5$ mm, $L_m = 1$ mm, $W_m = 0.5$ mm, $L_p = 3$ mm, $W_p = 3$ mm, $m = 0.2$ mm.

- Width of radiating patch, $W_p = \frac{c}{2f_r} \sqrt{\frac{2}{\epsilon_r + 1}}$
- Effective dielectric constant, $\epsilon_{eff} = \frac{\epsilon_r + 1}{2} + \frac{\epsilon_r - 1}{2} \left(1 + 12 \frac{h}{W_p}\right)^{-1/2}$
- Extension of patch length, $\Delta L = 0.412h \frac{(\epsilon_{eff} + 0.3)}{(\epsilon_{eff} - 0.258)} \left(\frac{W_p}{h} + 0.264\right)$
- Length of radiating patch, $L_p = L_{eff} - 2\Delta L$

Prasanna
 PRINCIPAL/DIRECTOR
 VIKAS GROUP OF INSTITUTIONS
 NUNNA - 521 212
 Vijayawada Rural, NTR Dist., A.F

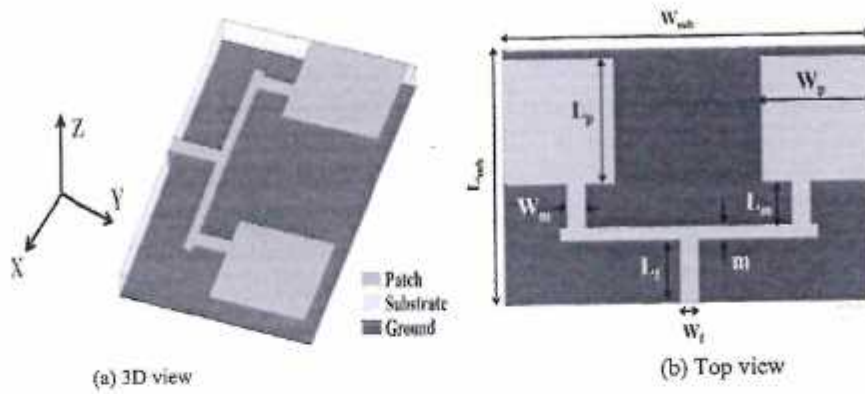


Fig. 1 Geometrical arrangement of 2-element array antenna composed with rectangular elements

$$\text{Where } L_{\text{eff}} = \frac{c}{2f_r \sqrt{\epsilon_{\text{eff}}}}$$

where 'c' is velocity of light = 3×10^8 m/s, ' f_r ' is resonant frequency, GHz and ' ϵ_r ' is dielectric constant of substrate = 2.2.

Reflection coefficient characteristics of designed 2-element array antenna loaded with rectangular elements are shown in Fig. 2. This suggested antenna obtains dual resonant frequencies at 30.05 GHz and 38.7 GHz having reflection coefficients of -24.35 dB and -23.30 dB, respectively. Impedance bandwidth of band-1 is 1.25 GHz over the operating frequency band of 29.37-30.62 GHz. Second band is achieved over the resonating band from 38.14 to 39.31 GHz, and its corresponding impedance bandwidth is 1.17 GHz. Obtained smaller impedance bandwidth ratios (IBR) of designed 2-element array antenna composed with rectangular elements are 4.16 and 3.02%. Voltage standing wave ratio (VSWR) characteristics of antenna represent the impedance matching condition in the entire bandwidth. An ideal value of VSWR is 1-∞. Figure 3 presents VSWR characteristics of designed antenna. VSWR values at resonant frequencies over operating band are 1.12 and 1.14. Group delay (t_{gd}) is

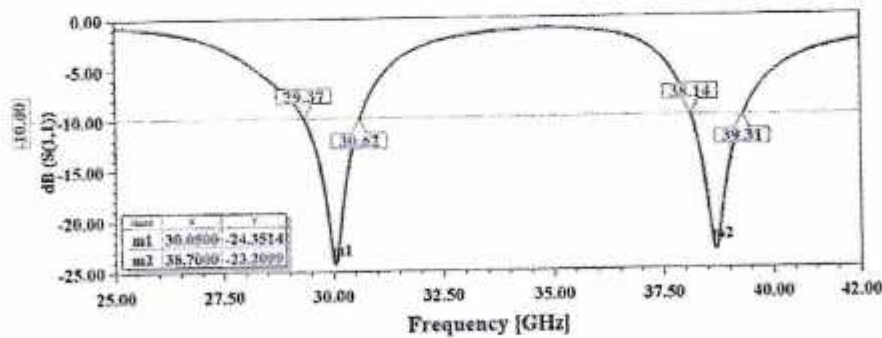


Fig. 2 Reflection coefficient characteristics of 2-element array antenna loaded with rectangular radiators

PKS 20/08

PRINCIPAL/DIRECTOR
 VIKAS GROUP OF INSTITUTIONS
 NUNNA - 521 212
 Vijayawada Rural, NTR Dist., A.P

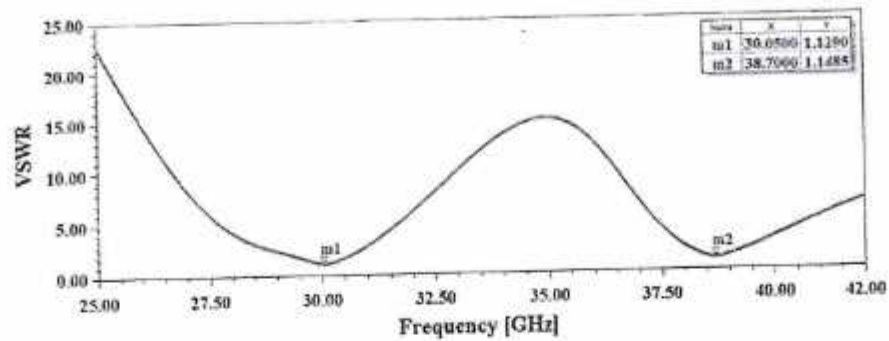


Fig. 3 VSWR characteristics of 2-element array antenna loaded with rectangular radiators

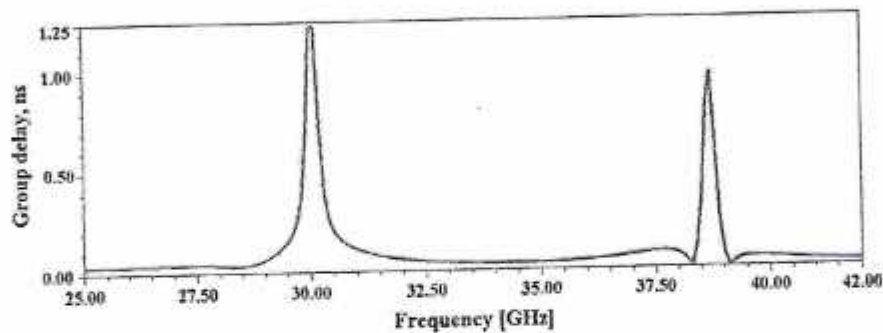


Fig. 4 Group delay plot of suggested 2-element array antenna loaded with rectangular radiators

a function of frequency, and it defines that the delay in electromagnetic (EM) signal reaches to receiver. Figure 4 shows the group delay characteristics of 2-element array antenna. Corresponding group delay values at resonant frequencies are 1.24 and 0.88 ns in the resonant bands.

Another important characteristic in antenna design is far-field reports such as 3D gain polar plots and radiation patterns. Maximum obtained peak gain values are 8.01 dBi at 30.05 GHz and 7.69 dBi at 38.7 GHz, and these 3D plots are shown in Fig. 5. The co-polarization and cross-polarization radiation patterns of designed antenna in H-plane (azimuthal plane) and E-plane (elevation plane) are simulated at ϕ (Φ) = 0° and 90° . Radiation patterns at 30.05 and 38.7 GHz in H-plane and E-plane are observed and are illustrated in Fig. 6. Figure 7 shows the surface current distribution of designed antenna at two resonant frequencies.

Prasanna

PRINCIPAL/DIRECTOR
VIKAS GROUP OF INSTITUTIONS
NUNNA - 521 212
Vijayawada Rural, NTR Dist., A.P

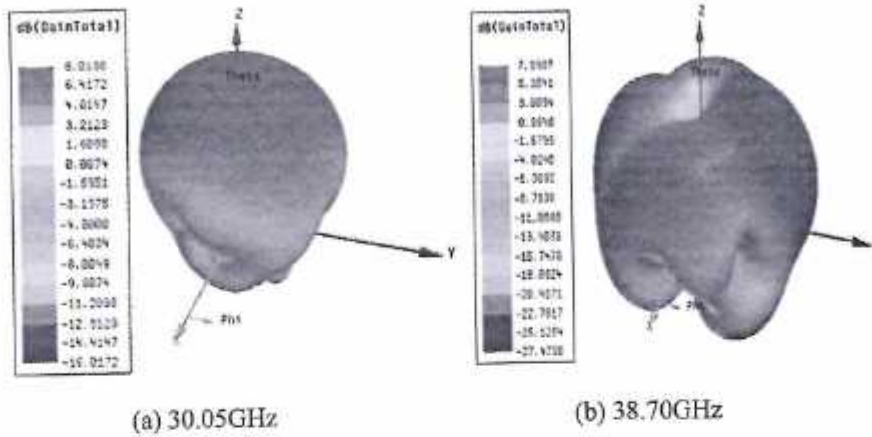


Fig. 5 3D gain polar plots of 2-element array antenna loaded with rectangular radiators

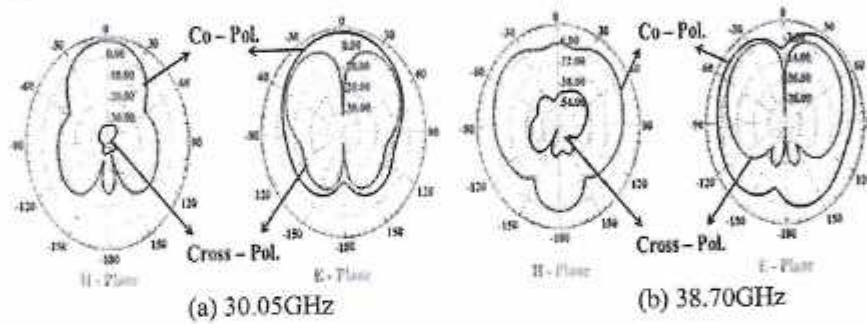


Fig. 6 Radiation patterns of suggested 2-element array antenna loaded with rectangular radiators

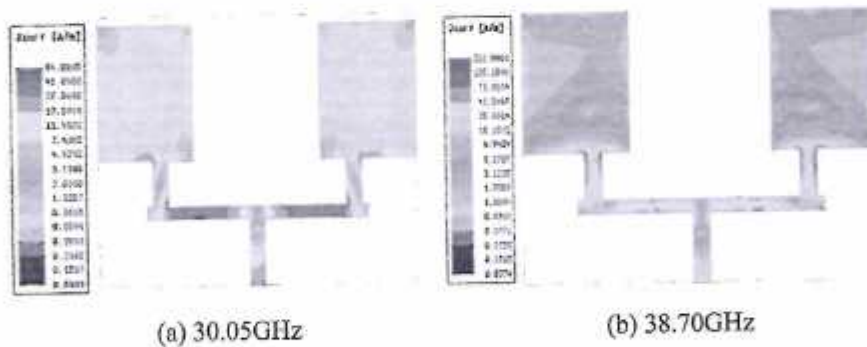


Fig. 7 Surface current distribution of designed antenna

Prasanna

PRINCIPAL/DIRECTOR
 VIKAS GROUP OF INSTITUTIONS
 NUNNA - 521 212
 Vijayawada Rural, NTR Dist., A.P

2.2 Design and Discussion About 2-Element Array Antenna Loaded with Octagon Radiators

In this section, rectangular radiating element is replaced with octagon radiating patch element. This octagon shape is looks near to circle shape. The dimension of octagon is derived from circular patch standard mathematical expressions. The geometry of circular patch is measured from standard mathematical equations [18]:

$$a = \frac{F}{1 + \frac{2h}{\pi F \epsilon_r} \left[\ln\left(\frac{\pi F}{2h}\right) + 1.7726 \right]^{\frac{1}{2}}}$$

where $F = \frac{8.791 \times 10^9}{f_r \sqrt{\epsilon_r}}$.

Radius of the circular patch is affected because of fringing field's variation in the microstrip design. So, the effective radius of circular patch antenna can be modified as

$$a_{\text{eff}} = a \left[1 + \frac{2h}{\pi a \epsilon_r} \left(\ln\left(\frac{2\pi}{ah}\right) + 1.7726 \right) \right]^{\frac{1}{2}}$$

The width of the feedline can be computed as $w_f = 8h \frac{e^A}{2A - 2}$

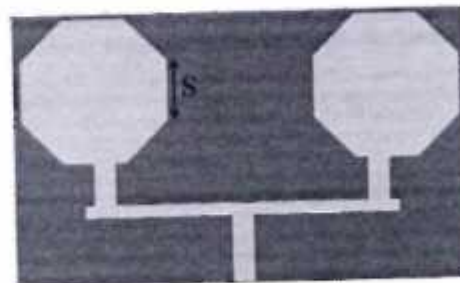
where $A = 2\pi \frac{Z_0}{Z_f} \sqrt{\frac{\epsilon_r + 1}{2}} + \frac{\epsilon_r - 1}{\epsilon_r + 1} \left(0.23 + \frac{0.11}{\epsilon_r} \right)$.

Z_0 Characteristic impedance of free space,
 Z_f Characteristic impedance of feedline.

Figure 8 shows the designed 2-element array antenna loaded with octagon patch elements. Optimized octagon edge (S) dimension is 1.34 mm. Figure 9 shows the reflection coefficient characteristics of designed 2-element array antenna, which is composed with octagon elements and is simulated using HFSS tool.

Figure 9 shows the return loss characteristics of designed antenna loaded with octagonal elements. This suggested antenna obtains dual resonant frequencies at 31 and 40.30 GHz, and its corresponding reflection coefficient value is

Fig. 8 Geometrical arrangement of 2-element array antenna loaded with octagon radiators



Prasanna
 PRINCIPAL/DIRECTOR
 VIKAS GROUP OF INSTITUTIONS
 NUNNA - 521 212
 Vijayawada Rural, NTR Dist., A.P.

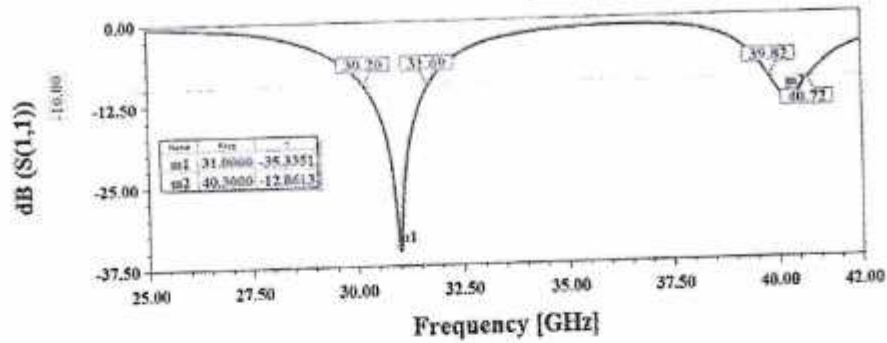


Fig. 9 Reflection coefficient characteristics of 2-element antenna array loaded with octagon radiators

- 35.33 and - 12.86 dB. Corresponding impedance bandwidths of dual bands are 1.49 GHz and 900 MHz. Band-1 covers from 30.20 to 31.69 GHz and 39.82 to 40.72 GHz. Smaller impedance bandwidth ratios at dual band resonant frequencies are 4.80% and 2.23%, respectively. Figure 10 demonstrates the VSWR plot of designed antenna loaded with octagon radiating elements. VSWR values at resonant frequencies are 1.03 at 31 GHz and 1.58 at 40.30 GHz. Group delay values at resonant frequencies are 2.05 ns and 0.2 ns at 31 GHz and 40.3 GHz, respectively, as shown in Fig. 11.

Figures 12 and 13 shows the far-field radiation characteristics of proposed 2-element array antenna composed of octagon elements. Figure 12 shows the 3D gain polar plots. Maximum obtained peak gain values at resonant frequencies are 9.54 dBi and 9.845 dBi, respectively. Figure 13 presents co-polarization and cross-polarization characteristics in H-plane and E-plane at phi values 0° and 90°. Figure 14 shows the surface current distribution of simulated antenna.

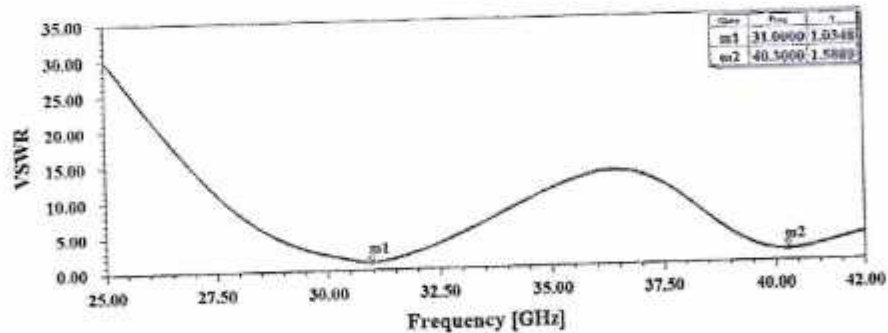


Fig. 10 VSWR characteristics of 2-element antenna array loaded with octagon radiators

PKS 20/08
 PRINCIPAL/DIRECTOR
 VIKAS GROUP OF INSTITUTIONS
 NUNNA - 521 212
 Vijayawada Rural, NTR Dist., A.P

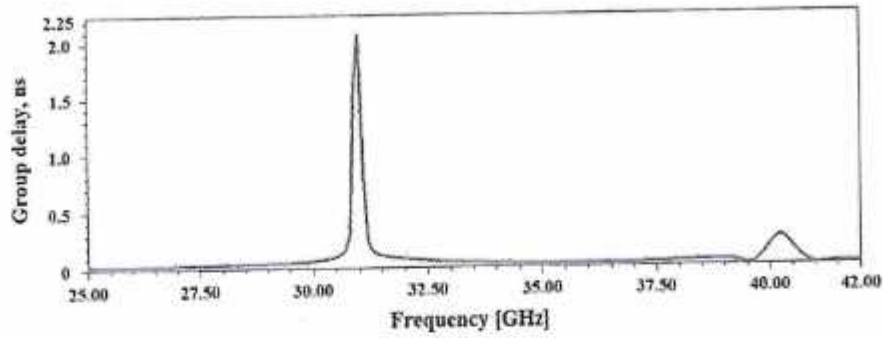


Fig. 11 Group delay plot of suggested 2-element antenna array loaded with octagon radiators

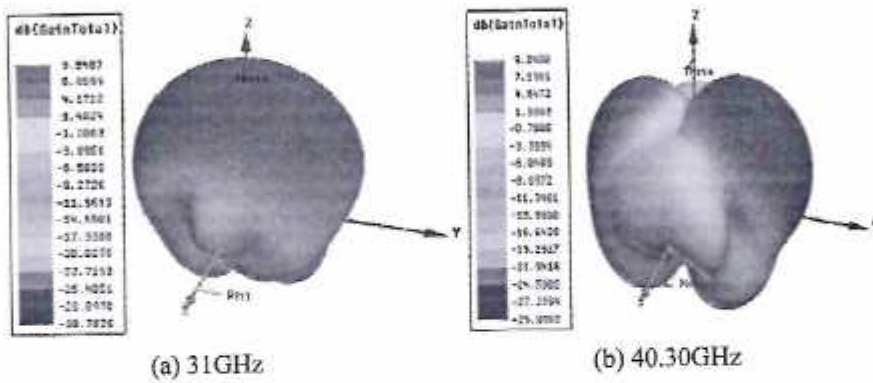


Fig. 12 3D gain plots of 2-element antenna array loaded with octagon radiators

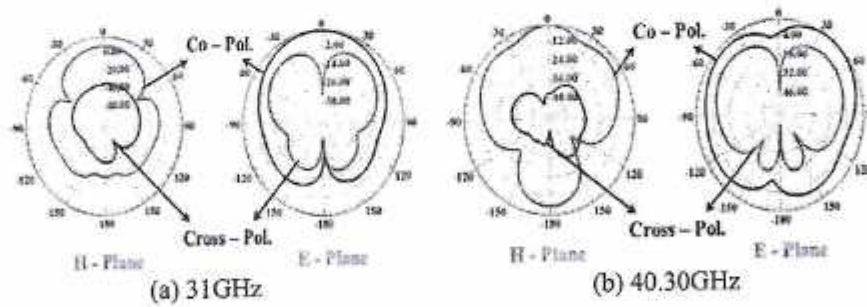


Fig. 13 Radiation patterns of 2-element antenna array loaded with octagon radiators

Prasanna
 PRINCIPAL/DIRECTOR
 VIKAS GROUP OF INSTITUTIONS
 NUNNA - 521 212
 Vijayawada Rural, NTR Dist., A.P

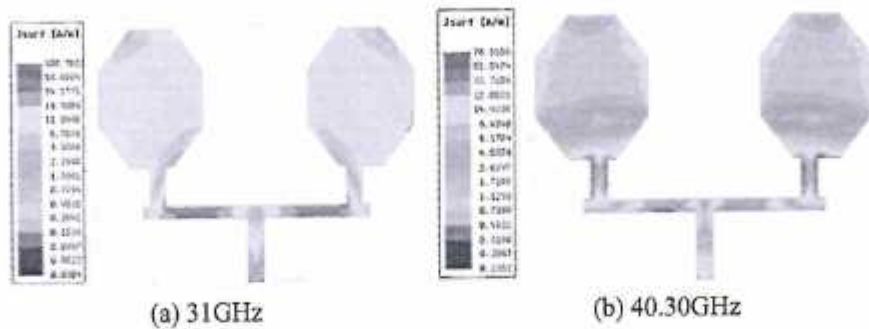
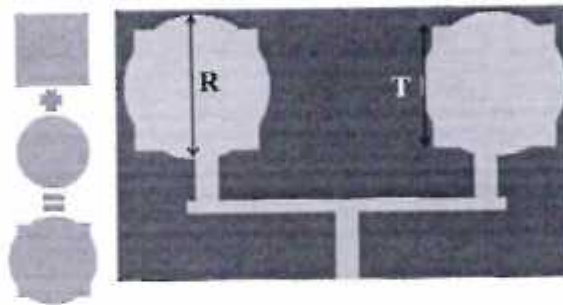


Fig. 14 Surface current distribution of 2-element array antenna loaded with rectangular radiators

Fig. 15 Geometrical arrangement of 2-element array antenna loaded with hybrid modeled radiators



2.3 Design and Discussion About 2-Element Array Antenna Loaded with Hybrid Elements

Figure 15 shows the hybrid-shaped elements loaded on 2-element array antenna. This hybrid shape is developed by combining rectangular and circular elements. The dimensions represented on presented antennas are $R = 3.2$ mm, $i = 2.7$ mm. These proposed antennas are simulated using HFSS tool and are printed on dielectric substrate material Rogers RT/Duroid 5880 (tm).

Figure 16 shows the reflection coefficient characteristics of 2-element array antenna loaded with hybrid-shaped element. This antenna resonates at two frequencies such as 30.90 and 39.8 GHz. Band-1 is resonating from 30.05 to 31.59 GHz and band-2 is resonating from 39.32 dB to 40.38 GHz. Impedance bandwidths at -10 dB are 1.54 GHz and 1.06 GHz, respectively, with S_{11} are -36.18 dB and -15.38 dB. Figure 17 shows the VSWR plot. VSWR values at resonant frequencies are 1.02 and 1.44. Figure 18 shows the group delay characteristics of designed antenna.

Figure 19 shows the 3D gain polar plots of designed antenna at two resonant frequencies such as 30.90 and 39.80 GHz. Maximum peak gain values of designed antenna are 8.96 dBi and 9.51 dBi at 30.90 GHz and 39.80 GHz, respectively. Figure 20 shows the radiation patterns of suggested antenna in terms of elevation and azimuthal planes. Figure 21 shows the surface current distribution of 2-element array antenna loaded with hybrid radiating elements.

Prasanna

PRINCIPAL/DIRECTOR
VIKAS GROUP OF INSTITUTIONS
NUNNA - 521 212
Vijayawada Rural, NTR Dist., A.P

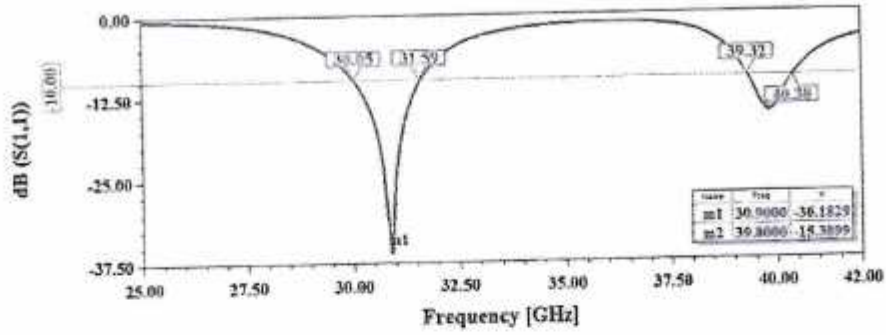


Fig. 16 Reflection coefficient characteristics of 2-element antenna array loaded with hybrid modeled radiators

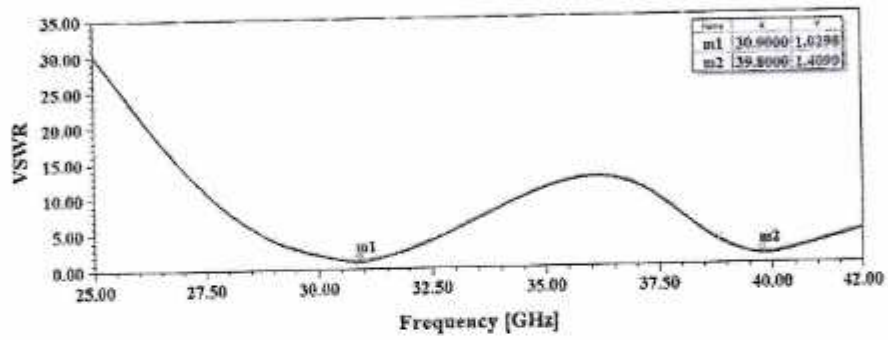


Fig. 17 VSWR characteristics of 2-element antenna array loaded with hybrid modeled radiators

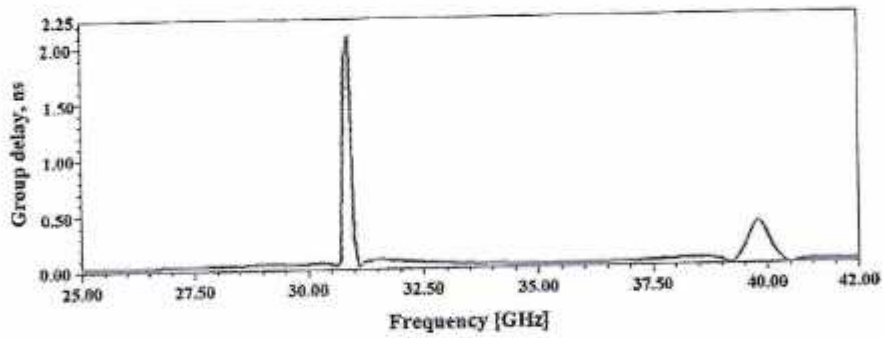


Fig. 18 Group delay plot of 2-element antenna array loaded with hybrid modeled radiators

DRS 20/12/20

PRINCIPAL/DIRECTOR
 VIKAS GROUP OF INSTITUTIONS
 NUNNA - 521 212
 Vijayawada Rural, NTR Dist., A.P

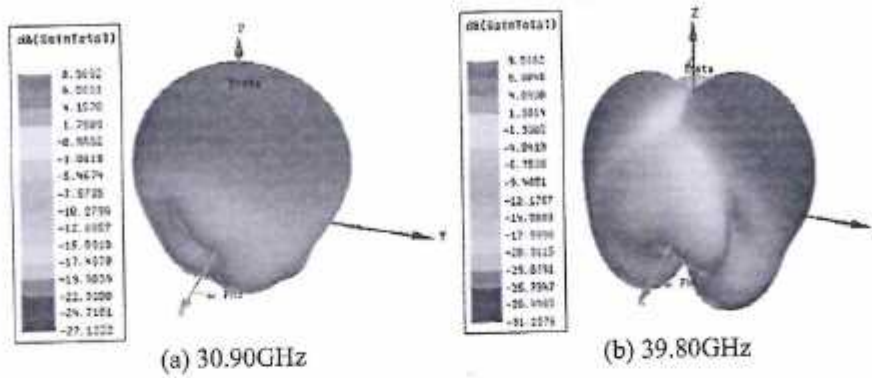


Fig. 19 3D gain plots of 2-element antenna array loaded with hybrid modeled radiators

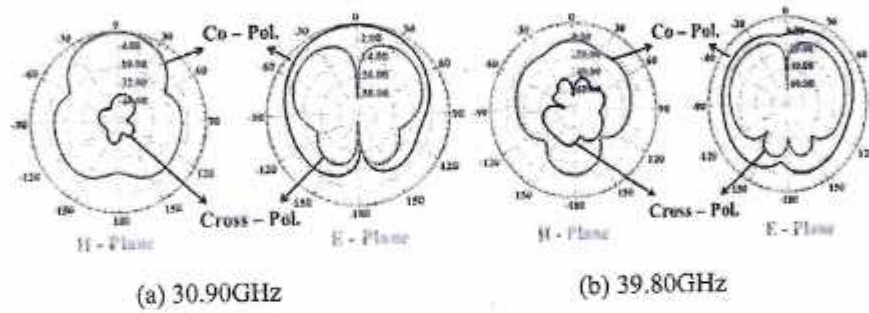


Fig. 20 Radiation patterns of 2-element antenna array loaded with hybrid modeled radiators

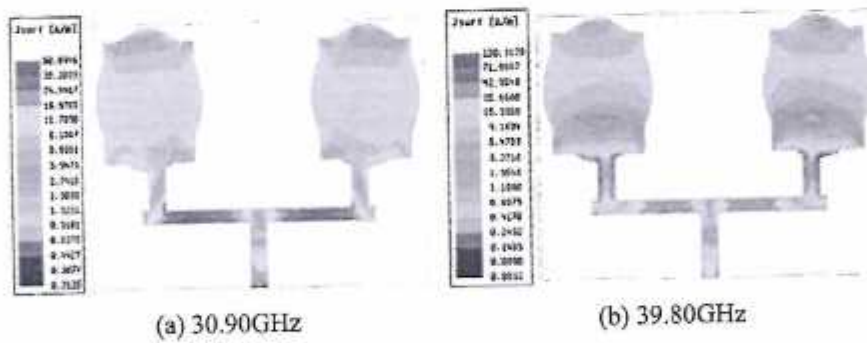


Fig. 21 Surface current distribution of designed antenna composed with hybrid modeled elements

Prasanna
 PRINCIPAL/DIRECTOR
 VIKAS GROUP OF INSTITUTIONS
 NUNNA - 521 212
 Vijayawada Rural, NTR Dist., A.P.

3 Design Summary of Designed Antennas

In this paper, 2-element array antennas are designed and simulated, which is loaded with rectangular elements, octagon elements and hybrid shape elements. Figures 22, 23 and 24 shows the reflection coefficient, VSWR and group delay responses for these three designed antennas. These three plots show the functional behavior on type of radiating element and its other parameters such as gain and fractional bandwidth ratios. Table 1 shows the comparison of designed antennas in terms of resonant frequency, reflection coefficient, bandwidth, gain, VSWR and group delay.

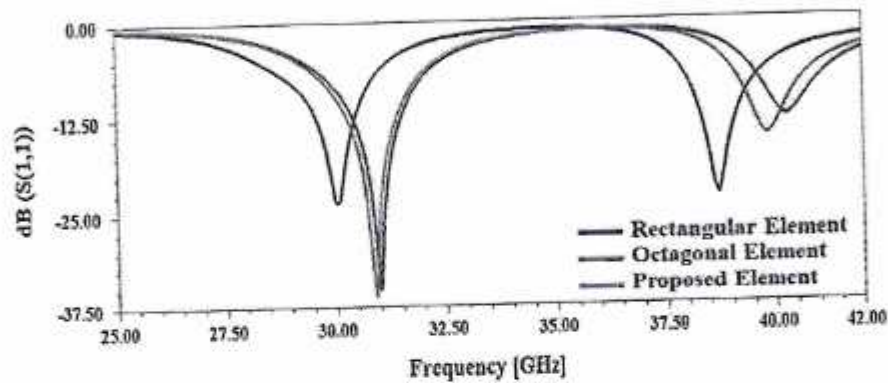


Fig. 22 Reflection coefficient characteristics of suggested 2-element antenna arrays

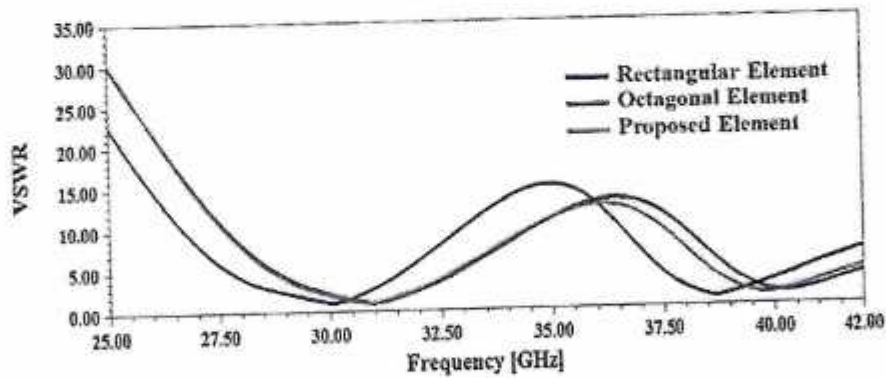


Fig. 23 VSWR characteristics of designed 2-element antenna arrays

DRS 2020

PRINCIPAL/DIRECTOR
VIKAS GROUP OF INSTITUTIONS
NUNNA - 521 212
Tayawada Rural, NTR Dist., A.P.

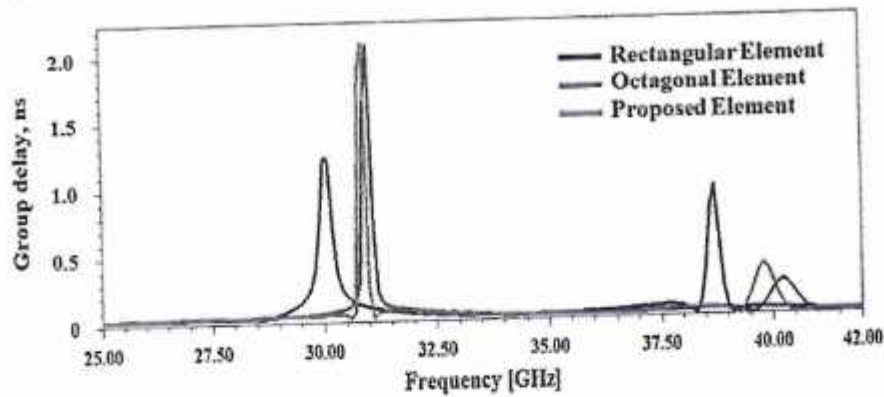


Fig. 24 Group delay plot of suggested 2-element array antenna

Table 1 Design summary of designed antennas analysis

Design	No. of bands	f_c , GHz	S_{11} , dB	BW, GHz	IBR, %	VSWR	Gain, dBi	Group delay (ns)
2-element array antenna composed rectangular radiator	2	30.05	-24.35	1.25	4.15	1.12	8.01	1.2
		38.70	-23.20	1.17	3.02	1.14	7.69	0.8
2-element array antenna composed octagon radiator	2	31.00	-35.33	1.49	4.80	1.03	9.54	2.05
		40.30	-12.86	0.90	2.23	1.58	9.84	0.25
2-element array antenna composed hybrid radiator	2	30.9	-36.18	1.54	4.98	1.02	8.96	2.1
		39.8	-15.38	1.06	2.66	1.40	9.51	0.3

4 Conclusion

A $10 \times 6 \text{ mm}^2$ compact 2-element array antennas has been designed in various configurations on Rogers RT/Duroid 5880 substrate material having dielectric constant of 2.2. These three antennas show dual band behavior in high-frequency Ka-band region, which are well suits for next-generation wireless applications. The reflection coefficient (S_{11}), voltage standing wave ratio (VSWR), group delay, 3D polar plots,

P. S. Rao

PRINCIPAL/DIRECTOR
VIKAS GROUP OF INSTITUTIONS
NUNNA - 521 212
Tayawada Rural, NTR Dist., A.P.

2D radiation patterns and surface current distributions are reported for all configurations in this article. On the basis of various antenna characteristics, 2-element array antenna loaded with hybrid radiator is appropriate for millimeter wave (mm wave), next-generation applications such as ultra-wide band (UWB), fifth generation communications and satellite systems.


References

1. Singh D, Choudhary SD, Mohapatra (2021) Design and fabrication of millimetre wave microstrip antenna for NGN application's. *Int J Microw Opt Technol* 16(3)
2. Li M, Luk K-M (2014) Low-cost wideband microstrip antenna array for 60-GHz applications. *IEEE Trans Antennas Propag* 62(6):3012–3018. <https://doi.org/10.1109/Tap.2014.2311994>
3. Choudhary SD, Srivastava A, Kumar M (2020) Design of single-fed dual-polarized dual-band slotted patch antenna for GPS And SDARS applications. *Microw Opt Technol Lett*:1–8
4. Ahmad W, Khan WT (2017) Small form factor dual band (28/38 GHz) PIFA antenna for 5G applications. In: 2017 IEEE MTT-S international conference on microwaves for intelligent mobility (ICMIM). <https://doi.org/10.1109/ICMIM.2017.7918846>
5. Xu J, Chen ZN, Qing X, Hong W (2011) Bandwidth enhancement for a 60 GHz substrate integrated waveguide fed cavity array antenna on LTCC. *IEEE Trans Antennas Propag* 59(3):826–832. <https://doi.org/10.1109/Tap.2010.2103018>
6. Goncharova I, Lindenmeier S (2017) A compact satellite antenna module for GPS, Galileo, GLONASS, Beidou and SDARS. In: Automotive application. 2017 11th European conference on antennas and propagation (EUCAP). <https://doi.org/10.23919/Eucap.2017.7928117>
7. Bai X, Qu S-W, Yang S, Hu J, Nie Z-P (2016) Millimeter-wave circularly polarized tapered-elliptical cavity antenna with wide axial-ratio beamwidth. *IEEE Trans Antennas Propag* 64(2):811–814. <https://doi.org/10.1109/Tap.2015.2507171>
8. Gautam AK, Kunwar A, Kanaujia BK (2014) Circularly polarized arrowhead-shape slotted microstrip antenna. *IEEE Antennas Wirel Propag Lett* 13:471–474. <https://doi.org/10.1109/Lawp.2014.2309719>
9. Nasimuddin ZNC, Qing X (2012) A compact circularly polarized cross-shaped slotted microstrip antenna. *IEEE Trans Antennas Propag* 60(3):1584–1588. <https://doi.org/10.1109/Tap.2011.3180334>
10. Li M, Luk K-M (2014) A wideband circularly polarized antenna for microwave and millimeter-wave applications. *IEEE Trans Antennas Propag* 62(4):1872–1879. <https://doi.org/10.1109/Tap.2014.2298246>
11. Wu T-Y, Chang T (2016) Interference reduction by millimeter wave technology for 5G-based green communications. *IEEE Access* 4:10228–10234. <https://doi.org/10.1109/Access.2016.2602318>
12. Balanis CA (2017) *Antenna theory*, 3rd edn. Wiley, New York, USA. ISBN: 978-1-118-64206-1
13. Luk K-M, Biqun W (2012) The magnetoelectric dipole—a wideband antenna for base stations in mobile communications. *Proc IEEE* 100(7):2297–2307. <https://doi.org/10.1109/Jproc.2012.2187039>
14. Hashem YAMK, Haraz OM, El-Sayed E-DM (2016) 6-element 28/38 GHz dual-band MIMO PIFA for future 5G cellular systems. In: 2016 IEEE international symposium on antennas and propagation (APSURSI). <https://doi.org/10.1109/Aps.2016.7695905>
15. Gautam PS, Singh D, Choudhary SD, Mohapatra B (2018) Design and comparison of multislot microstrip patch antenna for Wimax and WLAN application. In: 2018 international conference on advances in computing, communication control and networking (ICACCCN). <https://doi.org/10.1109/ICACCCN.2018.8748833>

PSR

PRINCIPAL/DIRECTOR
VIKAS GROUP OF INSTITUTIONS
NUNNA - 521 212
Vijayawada Rural, NTR Dist., A.P

16. Alvarez Outerelo D, Alejos AV, Garcia Sanchez M, Vera Isasa M (2015) Microstrip antenna for 5G broadband communications: overview of design issues. In: 2015 IEEE international symposium on antennas and propagation and USNC/URSI national radio science meeting. <https://doi.org/10.1109/Aps.2015.7305610>
17. Roh W, Seol J-Y, Park J, Lee B, Lee J, Kim Y, Cho J, Cheun K, Aryasfar F (2014) Millimeter-wave beamforming as an enabling technology for 5G cellular communications: theoretical feasibility and prototype results. *IEEE Commun Mag* 52(2):106–113. <https://doi.org/10.1109/Mcom.2014.6736750>
18. Murali Krishna C, Krishna Kanth Varma P, James Vijay P (2019) bandwidth enhancement of circular ring fractal antenna for wireless applications. In: Panda G, Satapathy S, Biswal B, Bansal R (eds) *Microelectronics, electromagnetics and telecommunications. Lecture notes in electrical engineering*, vol 521. Springer, Singapore. https://doi.org/10.1007/978-981-13-1906-8_31


PRINCIPAL/DIRECTOR
VIKAS GROUP OF INSTITUTIONS
NUNNA - 521 212
Vijayawada Rural, NTR Dist., A.P.